JACS
JOURNAL OF THE AMERICAN CHEMICAL SOCIETY

COMMUNICATION

pubs.acs.org/JACS

Microbots Swimming in the Flowing Streams of Microfluidic Channels

Samuel Sanchez,* Alexander A. Solovev, Stefan M. Harazim, and Oliver G. Schmidt

Institute for Integrative Nanosciences, IFW Dresden, Helmholtzstr. 20, D-01069 Dresden, Germany

Supporting Information

ABSTRACT: We describe the motion of self-propelled catalytic Ti/Fe/Pt rolled-up microtubes (microbots) in the microchannels of a microfluidics system. Their motion is precisely controlled by a small magnetic field, and the transport of multiple spherical microparticles into desired locations is achieved. The microbots are powerful enough to propel themselves against flowing streams. The integration of "smart and powerful" microbots into microchip systems can lead to multiple lab-on-a-chip functions such as separation of cells and biosensing.

The development of autonomous micro- and nanomachines capable of transporting cargoes in vitro in a rapid and controlled manner is of great interest in nanotechnology and fields ranging from drug delivery systems to biosensors and lab-on-a-chip applications. In eukaryotic cells, kinesin motors convert chemical energy from adenosine triphosphate (ATP) into mechanical energy to move intracellular cargo along microtubules where they "walk".[1] These "molecular shuttles" have motivated extensive research directed toward the effective transport of cargo and its controlled motion in vitro using microfluidic devices.[2] However, biomolecular motors have shown some downsides when used outside of their natural environments, such as low power for transporting colloidal cargo and inherent instability.[3] The easy loading and delivery of cargo within a lab-on-a-chip microchannel network remains a big challenge for this class of nanomotors, motivating the search for versatile nanomachines that can swim under diverse conditions while transporting cargo in a controlled manner.

The self-propulsion of artificial micro- and nanomachines associated with the catalytic decomposition of hydrogen peroxide has been subject of increasing interest over the last five years.[4] The motion of the artificial catalytic nanomachines is commonly studied in a free bulk solution, which nonetheless differs significantly from the streamlike channel networks existing in the human body, for example. In particular, only one precedent reported the motion of nanomotors within microfluidic channels, wherein their speed was dramatically reduced and the transport of single cargo was hence limited because of the low developed power.[5] In addition, like molecular motors, bimetallic nanomotors rely on specialized interactions with the cargo to load the particles, such as magnetic forces,[5] streptavidin−biotin linkage,[6] or electrostatic forces.[6] We recently reported the loading, transport, and delivery of several microobjects[7] and cells[8] in free solution by using rolled-up tubular microjet engines (dubbed "microbots"). Microtubes containing a Pt catalyst[9] or catalase enzymes[10] in their inner layer can trigger the breakdown of the hydrogen peroxide fuel wherein they are immersed. The hollow structure generates a thrust of oxygen microbubbles in their interior that is released from one of the tubular openings. The motion of laminar fluid through the interior of the microtube sucks the cargo toward its front opening, permitting a large variety of microobjects to be easily transported without the need of functionalization.[7] Although the performance of these microbots was well-demonstrated, their motion in microfluidic channels has not been reported to date.

Herein we present the controlled motion of Ti/Fe/Pt rolled-up microtubes in the microchannels of a microfluidics system and the transport of multiple spherical microparticles into desired locations. The microbots exhibit velocities similar to those in free bulk solution, and their motion is controlled by an external magnetic field. We also report for the first time the motion of artificial micromachines against and along flowing streams.

The accurate stirring of autonomous microbots swimming within polydimethylsiloxane (PDMS) microfluidic channels is shown in Figure 1 (also see video 1 in the Supporting Information). First, the Ti/Fe/Pt microbots were suspended along with polystyrene microparticles (5 μm diameter) in a reservoir chamber (1 cm^2) containing hydrogen peroxide solution (8.75% v/v) and soap (5% v/v). Immediately, each microbot started to be self-propelled by the oxygen released from one of the openings of the microtube, as described elsewhere.[7,9,11] The optical images in Figure 1 depict a microbot traveling and being directed from the wide microfluidic channel (Figure 1A) toward the narrower "working" areas (Figure 1B,C) wherein microparticles were ultimately loaded and transported. The oxygen bubbles released from the microbots' tails are usually helpful in visualizing their trajectories along the microchip. It is important to note that here a high concentration of soap (5% v/v) was used to reduce the size of the bubbles, which otherwise would expand and block the channels. The microbot faced the entrance of the microchannel (Figure 1B) and then followed a straight trajectory achieved while the magnetic field was kept stationary (Figure 1 C). As an example, a microbot against a flow of 73 μm s^{-1} traveled at 78 μm s^{-1} for an average of 13 s (see videos 1 and 2). This speed significantly overcame Brownian motion, proving a high power output from the rolled-up microbots into the fabricated microchannels. It should be noted that in all of these experiments, we made use of tracer polystyrene particles with diameters of 5 μm to correlate the flow rate. The microbots' motion was controlled by a magnetic field generated by a small NdFeB magnet bar placed underneath the microfluidic chip. Video 3 shows the motion of several microbots in peroxide solution controlled by using a conventional joystick that was programmed via a Labview interface.

Received: October 26, 2010
Published: December 17, 2010

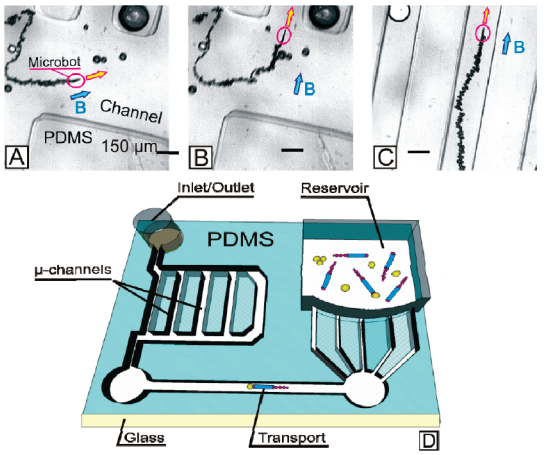

Figure 1. (A−C). Optical sequence of a microbot "swimming" into the microchannels of a PDMS chip. The blue arrow represents the direction of the magnetic field. (D) Schematic of the fabricated microchip used for the transport of microparticles.

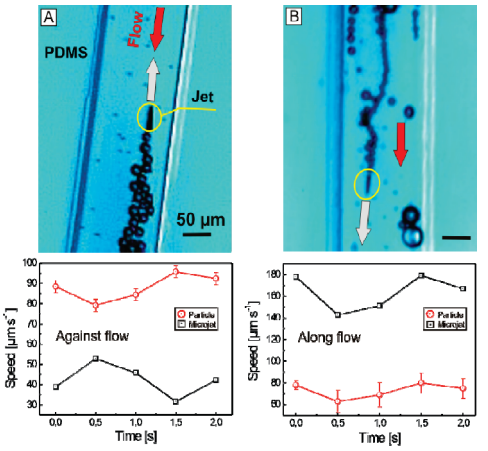

Figure 2. Microbots swimming (A) against and (B) along the continuous induced flow of fuel into the microchannels. The plots at the bottom depict the speed of the tracer particles ($n = 5$) and the microbots in absolute values.

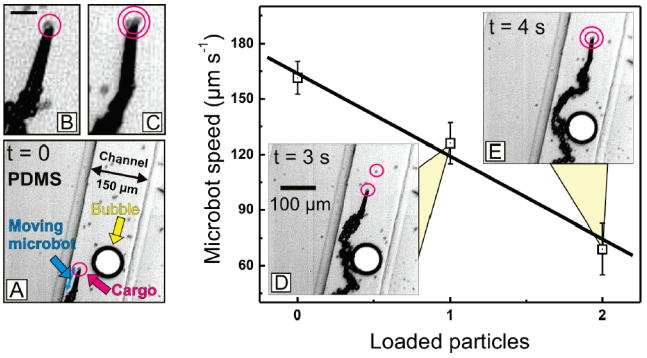

Figure 3. Catalytic Ti/Fe/Pt microbot loading and transporting 5 μm diameter polystyrene particles into microfluidic channels. The plot shows the dependence of the microbot speed on the number of particles loaded. (A) Moving microbot sorting a residual bubble into a 150 μm wide microchannel in a PDMS microchip. (B, C) Zoomed images of the microbot loading (B) one and (C) two microparticles. (D, E) Microbot transporting (D) one and (E) two microparticles into the microchannels.

The joystick controlled a stepping motor in which the magnet bar was fixed, thereby setting the direction of the microbots' motion. Video 3 clearly demonstrates local and precise steering of several microbots synchronized with the rotational magnetic field. As a particular example, video 4 illustrates the rotation of a static microtube located in a microfluidic channel containing distilled water. Thus, the multiple and individual steering of microbots, either in free bulk solution and/or in microchannels with spatial precision is possible.

A reduction in the speed of nanomotors propelled into PDMS microchannels relative to that of nanomotors in free solution was previously reported. The authors hypothesized that thhis was caused by absorption of the stationary H_2O_2 into the PDMS matrix.[5] To overcome the possible absorption of fuel, we introduced a flow of hydrogen peroxide solution into the microchip chamber that allows at the same time a continuous supply of the fuel to the microbots. Intensive research has been carried out in the search for a high power output, which is translated to high propulsion speeds with modifications in the surface of the motors[12] and the fuel composition.[13] In order to study whether our microbots were able to produce enough propulsion power by themselves without further alterations, we directed them against flowing streams, as shown in Figure 2A. The laminar flow in the microchannels had a parabolic profile[14] (i.e., the flow was faster at the center than at the edges). This phenomenon can be observed in the motion of the particles shown in video 5. Thus, all of the represented data points in Figure 2 correspond to particles moving near the microbot in the center of the microchannel. Also, we navigated the microbot to the center of the channels to obtain either the maximal propulsion or the maximal drag force. As expected, the increase in the flow rate (and thus a higher hydrodynamic drag force) induced a reduction in the motion of the microbots, whose speed droped from 50 to 30 μm s^{-1} as the flow rate increased from 80 to 100 μm s^{-1} in the opposite direction (Figure 2A and video 5). In addition, a microbot moving along (i.e., in the same direction as) the flow accelerated, acquiring speeds ranging from 140 to 180 μm s^{-1} (Figure 2B and video 6). The ability of artificial micromachines to swim against a continuous flow is of particular interest for future applications, since living systems contain moving fluids rather than static ones.

The transport of cargo in a controlled manner within microfluidic channels is of great importance in lab-on-a-chip applications and (bio)chemical separations. We studied the loading of microparticles into microchannels, as represented in Figure 3. The speed of the microbot decreased with the number of particles loaded; nevertheless, the microbot was able to load two consecutive particles, one after another (video 7). The transport of multiple particles in microchannels has not been reported previously. The microbot swam at a speed of ~160 μm s^{-1} when free of cargo and decelerated linearly as more particles were loaded. The pickup of the first particle is shown in Figure 3A,B. The microbot then swam for 3 s toward a second particle (Figure 3D), which was loaded in the same fashion once it was close enough to the mouth of the microtube (Figure 3E). At this point, the speed was reduced from 125 μm s^{-1} with one particle loaded (see zoomed image in Figure 3B) to 72 μm s^{-1} when transporting two particles (zoomed images in Figure 3B,C). The reduction in speed is attributed to two reasons: (i) the increase in the drag force with increasing number of particles transported and (ii) the partial blocking of the entrance of the tube by the loaded particles, which might reduce the fluid pumping and therefore the propulsion.

The drag force for a single spherical particle at low Reynolds numbers can be calculated using the Stokes equation. The equivalent

dx.doi.org/10.1021/ja109627w | J. Am. Chem. Soc. 2011, 133, 701–703

microbot force for pushing a single 5 μm diameter particle was calculated to be $F_{\mu bot}$ = 7.3 pN.

In summary, we have demonstrated the ability of catalytic microbots to swim in a controllable manner within microfluidic channels. The Ti/Fe/Pt rolled-up microbots are powerful enough to propel themselves through flowing streams. Accurate motion control, high propulsion power, and the pumping mechanism of motion permit the microbots to easily load multiple cargoes and transport them to desired locations in the microfluidic chip. The integration of "smart and powerful" microbots with different microchip schemes can lead to multiple functions in lab-on-a-chip devices, such as the separation and sorting of drugs or cells as well as biosensing. This combination will allow for the understanding of collective behaviors such as nonbiological chemotaxis.

■ ASSOCIATED CONTENT

Supporting Information. Experimental section, reagents, additional figures, additional discussion, and videos of microbots (AVI). This material is available free of charge via the Internet at http://pubs.acs.org.

■ AUTHOR INFORMATION

Corresponding Author
s.sanchez@ifw-dresden.de

■ ACKNOWLEDGMENT

This work was supported by a grant from the Volkswagen Foundation (I/84 072). The authors thank E. J. Smith for comments on the manuscript.

■ REFERENCES

(1) Van den Heuvel, M. G. L.; Dekker, C. *Science* **2007,** *317,* 333–336.

(2) (a) Clemens, J.; Hess, H.; Howard, J.; Vogel, V. *Langmuir* **2003,** *19,* 1738–1744. (b) Van den Heuvel, M. G. L.; de Graaff, M. P.; Dekker, C. *Science* **2006,** *312,* 910–914. (c) Hess, H.; Matzke, C. M.; Doot, R. K.; Clemmens, J.; Bachand, G. D.; Bunker, B. C.; Vogel, V. *Nano Lett.* **2003,** *3,* 1651–1655.

(3) Browne, W. R.; Feringa, B. L. *Nature* **2006,** *1,* 25–35.

(4) (a) Paxton, W. F.; Sundararajan, S.; Mallouk, T. E.; Sen, A. *Angew. Chem., Int. Ed.* **2006,** *45,* 5420–5429. (b) Mallouk, T. E.; Sen, A. *Sci. Am.* **2009,** *300,* 72–77. (c) Wang, J. *ACS Nano* **2009,** *3,* 4–9. (d) Sanchez, S.; Pumera, M. *Chem.—Asian J.* **2009,** *4,* 1402–1410. (e) Mirkovic, T.; Zacharia, N. S.; Scholes, G. D.; Ozin, G. A. *Small* **2010,** *6,* 159–167. (f) Pumera, M. *Nanoscale* **2010,** *2,* 1643–1649. (g) Sen, A.; Ibele, M.; Hong, Y.; Velegol, D. *Faraday Discuss.* **2009,** *143,* 15–27. (h) Mirkovic, T.; Zacharia, N. S.; Scholes, G. D.; Ozin, G. A. *ACS Nano* **2010,** *4,* 1782–1789.

(5) Burdick, J.; Laocharoensuk, R.; Wheat, P. M.; Posner, J. D.; Wang, J. *J. Am. Chem. Soc.* **2008,** *130,* 8164–8165.

(6) Sundararajan, S.; Lammert, P. E.; Zudans, A. W.; Crespi, V. H.; Sen, A. *Nano Lett.* **2008,** *8,* 1271–1276.

(7) Solovev, A. A.; Sanchez, S.; Pumera, M.; Mei, Y. F.; Schmidt, O. G. *Adv. Funct. Mater.* **2010,** *20,* 2430–2435.

(8) Sanchez, S.; Solovev, A. A.; Schulze, S.; Schmidt, O. G. *Chem. Commun.* **2011,** *47,* 698–700.

(9) Solovev, A. A.; Mei, Y. F.; Bermudez Urena, E.; Huang, G. S.; Schmidt, O. G. *Small* **2009,** *5,* 1688–1691.

(10) Sanchez, S.; Solovev, A. A.; Mei, Y. F.; Schmidt, O. G. *J. Am. Chem. Soc.* **2010,** *132,* 13144–13145.

(11) Mei, Y. F.; Huang, G. S.; Solovev, A. A.; Bermudez Urena, E.; Monch, I.; Ding, F.; Reindl, T.; Fu, R. K. Y.; Chu, P. K.; Schmidt, O. G. *Adv. Mater.* **2008,** *20,* 4085–4090.

(12) (a) Zacharia, N. S.; Sadeq, Z. S.; Ozin, G. A. *Chem. Commun.* **2009,** 5856–5858. (b) Demirok, U. K.; Laocharoensuk, R.; Manesh, K. M.; Wang, J. *Angew. Chem., Int. Ed.* **2008,** *47,* 9349–9351.

(13) Laocharoensuk, R.; Burdick, J.; Wang, J. *ACS Nano* **2008,** *2,* 1069–1075.

(14) Geschke, O.; Klank, H.; Telleman, P. *Microsystem Engineering of Lab-on-a-Chip Devices,* 2nd ed.; Wiley-VCH: Weinheim, Germany, 2008.